

Supplementary Information

Robust Long-Range Coordination of Spontaneous Neural Activity in Waking, Sleep and Anesthesia

Xiao Liu^{1*}, Toru Yanagawa², David A. Leopold³, Naotaka Fujii², and Jeff H. Duyn¹

¹Advanced MRI Section, Laboratory of Functional and Molecular Imaging,
National Institute of Neurological Disorders and Stroke,
National Institutes of Health, Bethesda, MD, USA;

²Laboratory for Adaptive Intelligence, Brain Science Institute,
RIKEN 2-1 Hirosawa, Wako, Saitama, Japan;

³Section on Cognitive Neurophysiology and Imaging, Laboratory of Neuropsychology,
National Institute of Mental Health,
National Institutes of Health, Bethesda, MD, USA

* Corresponding Author: Xiao Liu, PhD
10 Center Dr.

Bldg. 10, Rm. B1D-723A - MSC 1065

Bethesda, MD 20892-1065, USA

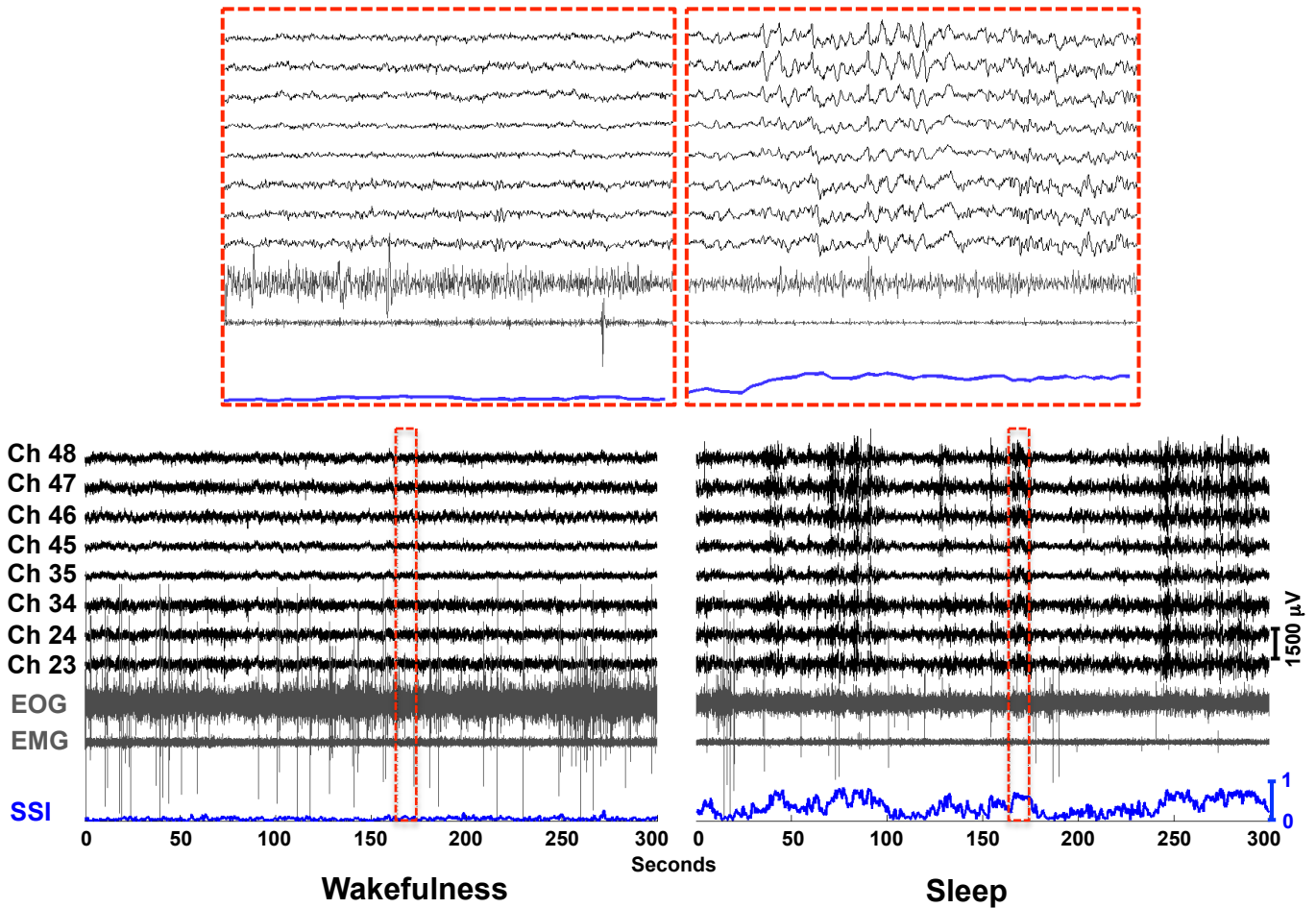
Tel.: +1 301 594 7312

Fax: +1 301 480 1981

E-mail: liux15@ninds.nih.gov

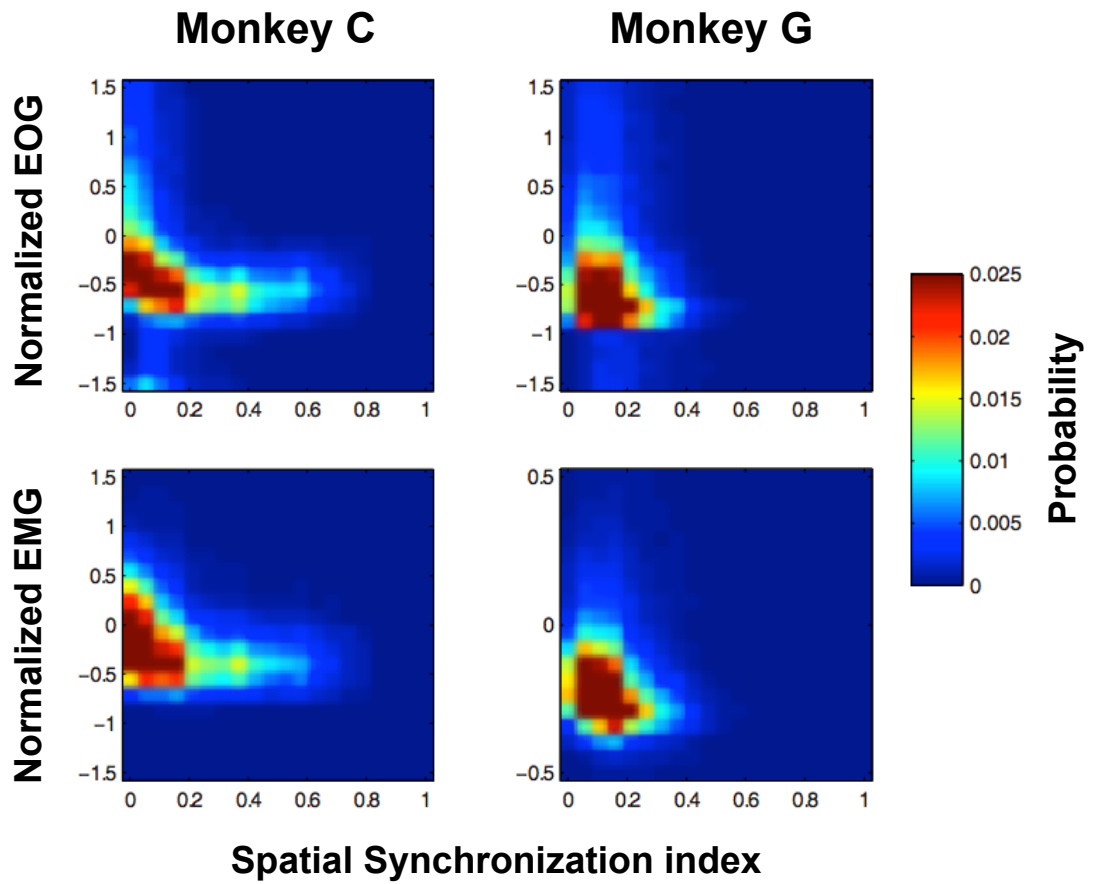
Supplementary Table 1 Experiment Summary

Experiment Date	Monkey	Conditions	# of Sessions
20110621	C	Eyes-Closed \ Ketamine	3 \ 3
20110622	C	Eyes-Closed \ Ketamine	3 \ 3
20120730	C	Eyes-Closed \ Propofol	3 \ 1
20120802	C	Eyes-Closed \ Propofol	3 \ 2
20120705	C	Eyes-Closed \ Sleep	1 \ 3
20120706	C	Eyes-Closed \ Sleep	1 \ 2
20120710	C	Eyes-Closed \ Sleep	1 \ 1
20101111	G	Eyes-Closed \ Ketamine	3 \ 2
20101112	G	Eyes-Closed \ Ketamine	3 \ 2
20120731	G	Eyes-Closed \ Propofol	3 \ 1
20120803	G	Eyes-Closed \ Propofol	3 \ 1
20120712	G	Eyes-Closed \ Sleep	1 \ 1
20120713	G	Eyes-Closed \ Sleep	2 \ 2
20110513	K	Eyes-Closed \ Ketamine	3 \ 2
20110524	K	Eyes-Closed \ Ketamine	3 \ 3
20110525	K	Eyes-Closed \ Ketamine	3 \ 3
20110523	S	Eyes-Closed \ Ketamine	3 \ 2
20110526	S	Eyes-Closed \ Ketamine	3 \ 2
20110527	S	Eyes-Closed \ Ketamine	3 \ 2
20110607	S	Eyes-Closed \ Ketamine	2 \ 2



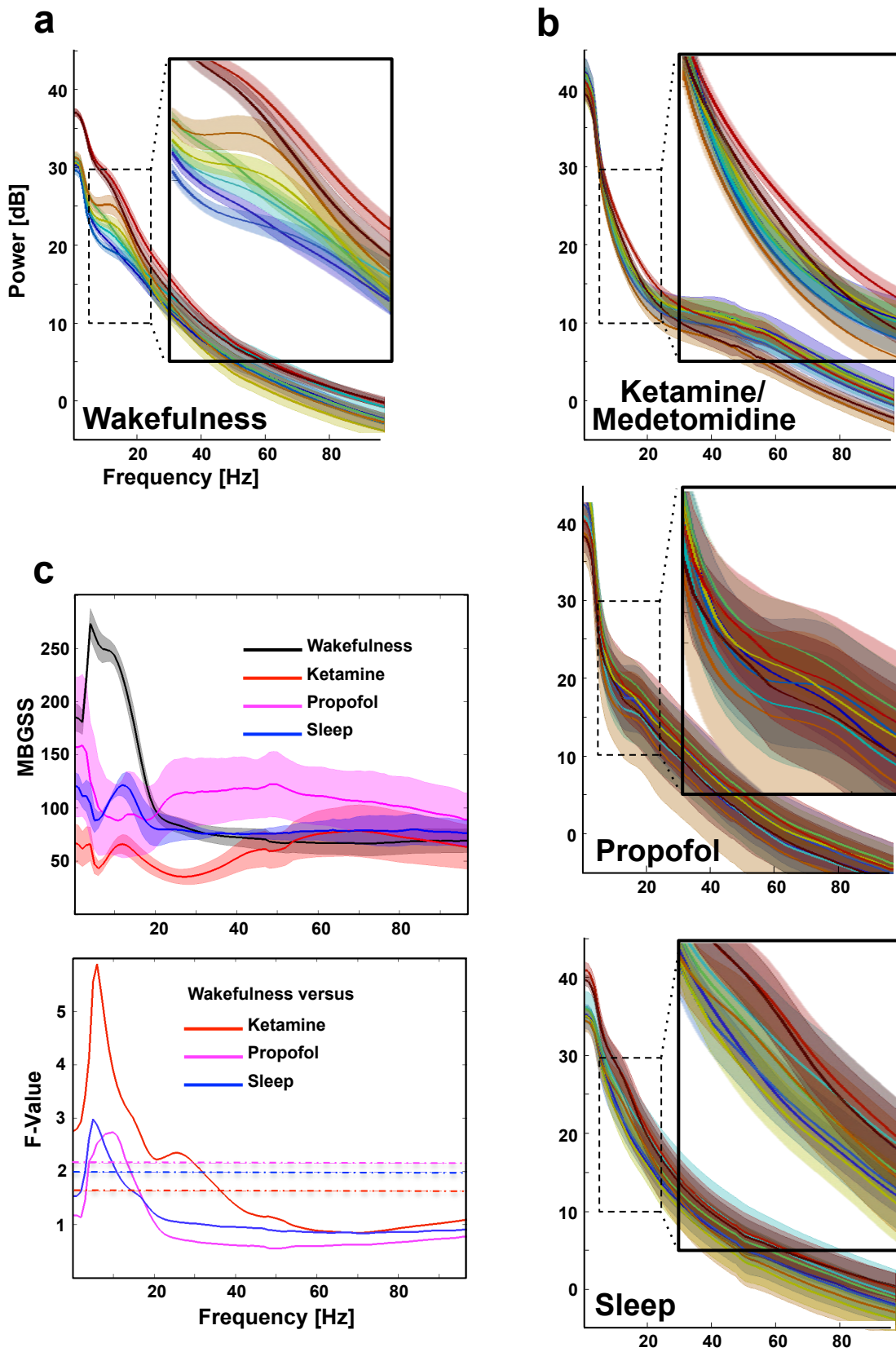
Supplementary Fig. 1

ECoG, electrooculography (EOG), and electromyography (EMG) recorded during typical eyes-closed (left) and sleep (right) sessions from Monkey C, as well as the corresponding spatial synchronization index (SSI). The sleep session is characterized by the intermittent, large amplitude slow wave activity, reduced eye movement and muscle tone, and significantly higher sleep scores. A 10-second segment is selected and zoomed in for each session.



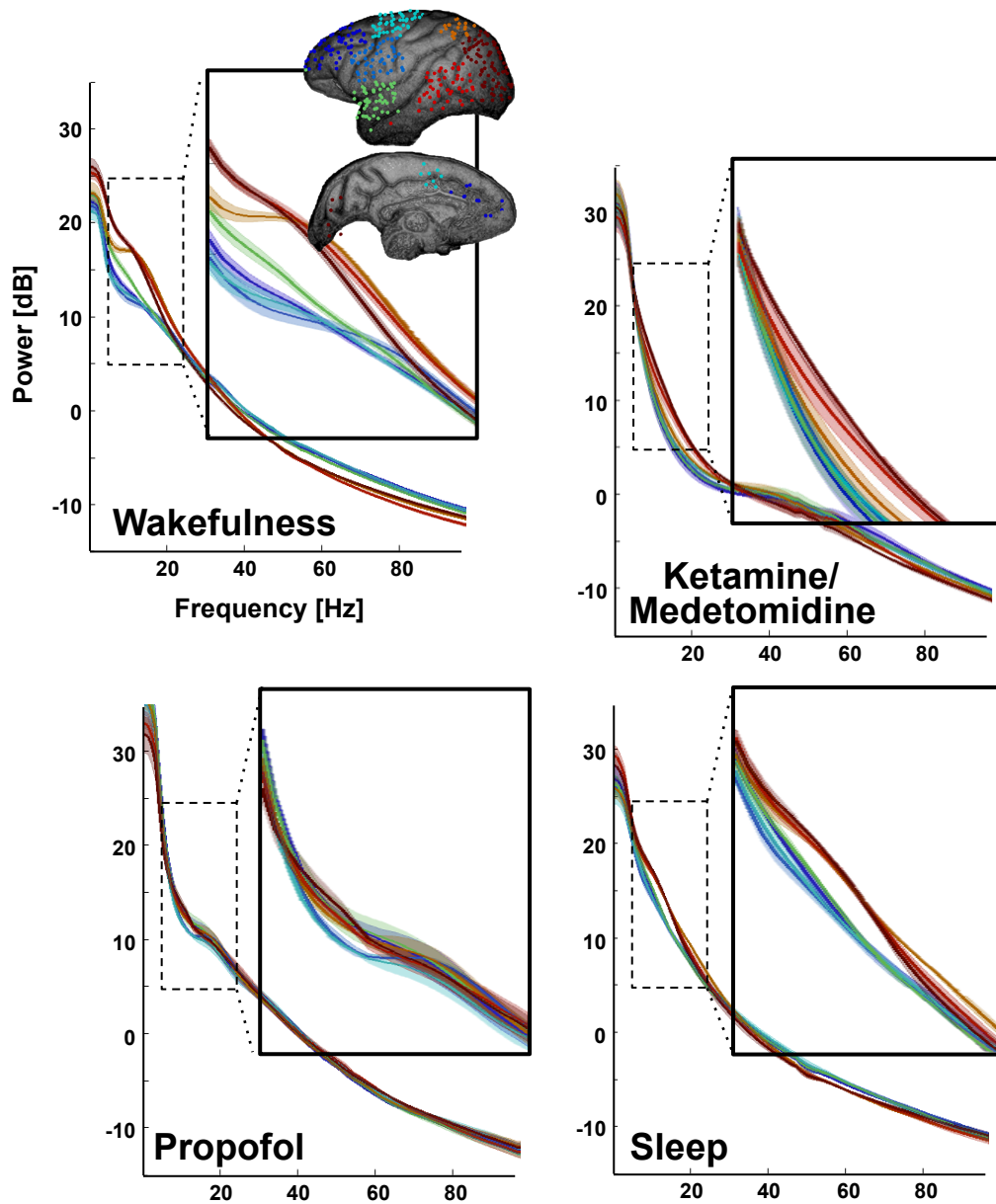
Supplementary Fig. 2

Two-dimensional histogram of the spatial synchronization of *d*-band power and normalized EOG or EMG. The raw EOG and EMG signals were converted to absolute value and were averaged in each 1 sec time bin. The averaged EOG and EMG were centered and scaled by using the mean and standard deviation along the time bin (Normalized EMG and EOG).



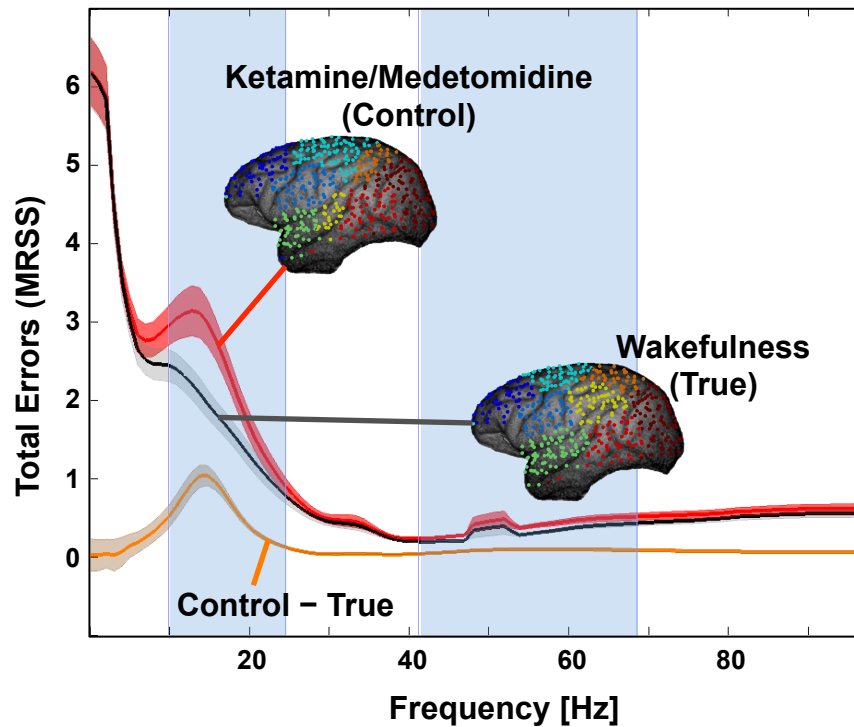
Supplementary Fig. 3

Power spectra without the mean subtraction. The analysis in **Fig 5** was repeated without subtracting the mean from each spectrum. All others are the same as those specified in **Fig 5**.



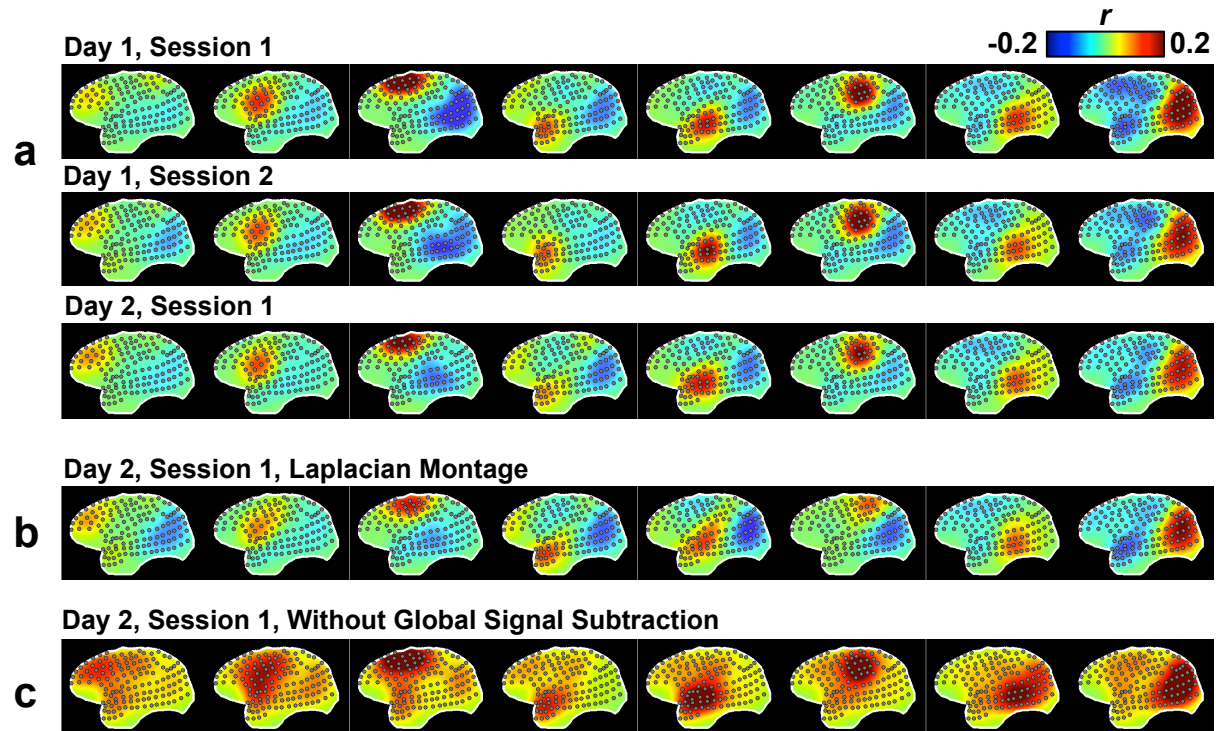
Supplementary Fig. 4

Power spectra averaged based on a fixed network parcellation. The analysis in **Fig 5** was repeated using a fixed network parcellation that combines those under the eyes-closed and ketamine/medetomidine conditions. All others are the same as those specified in **Fig 5**.



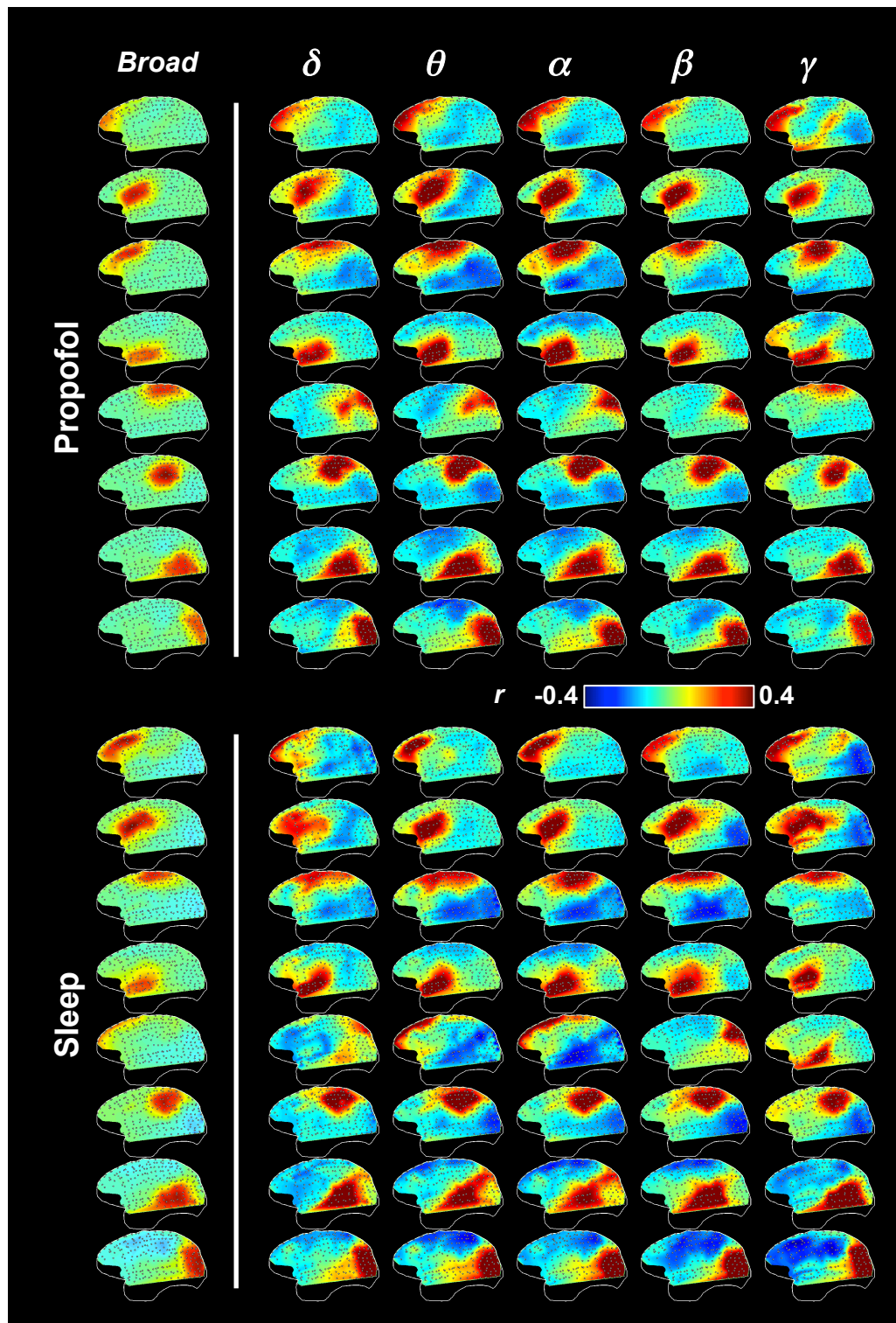
Supplementary Fig. 5

A comparison of two network-parcellation models in describing the network-specific organization of the power spectra. The demeaned power spectra of the eyes-closed wakefulness were fitted into the network parcellations of the same condition (true model) and ketamine/medetomidine anesthesia (control model), both of which show similar, anteroposterior arrangement of the networks. The mean residual-sum-of-squares (MRSS), quantifying within-network differences in power spectra, is much smaller (mainly within a-b frequency range) for the true model (black line) than for the control model (red line). The differences are statistically significant ($p < 0.001$, Bonferroni corrected) for a range of frequencies (light blue shadows). Shadows in other colors represent areas within one S.E.M. across experiments ($n = 20$). The results suggests that regional specificity of the power spectra follows the topographic distribution of the networks, since rearranging electrodes in a slightly different way resulted in a significant reduction in within-group similarity of the spectra.



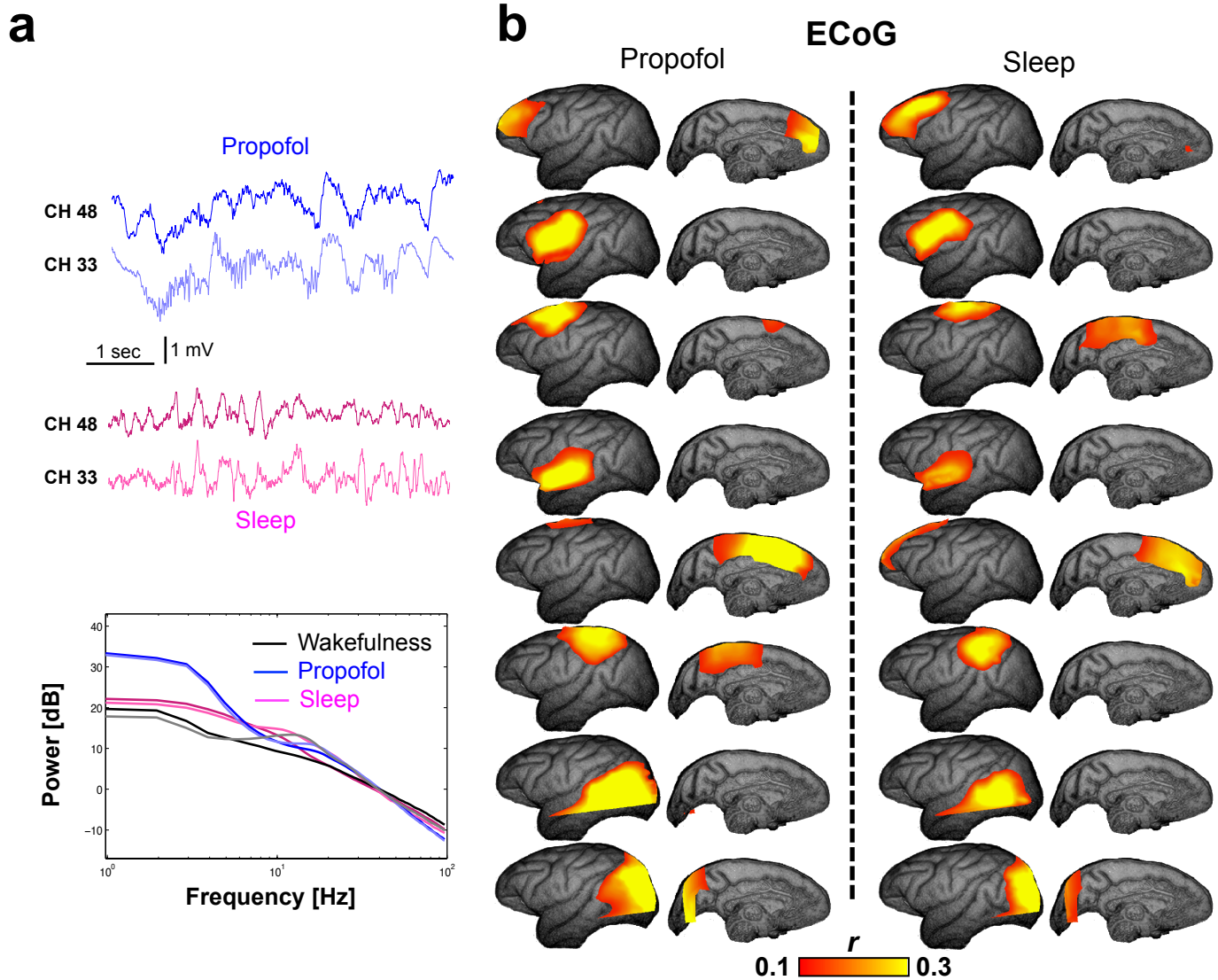
Supplementary Fig. 6

ECoG correlation structures are stable across sessions and experiments, and insensitive by certain pre-processing steps. (a) Spatial patterns of broadband ECoG power co-variation in 5-minute sessions acquired from Monkey S in the same experiment or at different days. (b) Laplacian montage is applied to one above session in the substitution of the average re-reference method, but the clustering-based correlation analysis resulted in very similar clusters. (c) The correlation analysis was also applied to the same session without subtracting the global power variation averaged across electrodes. Although the correlation strength increased globally, the spatial patterns remain similar.



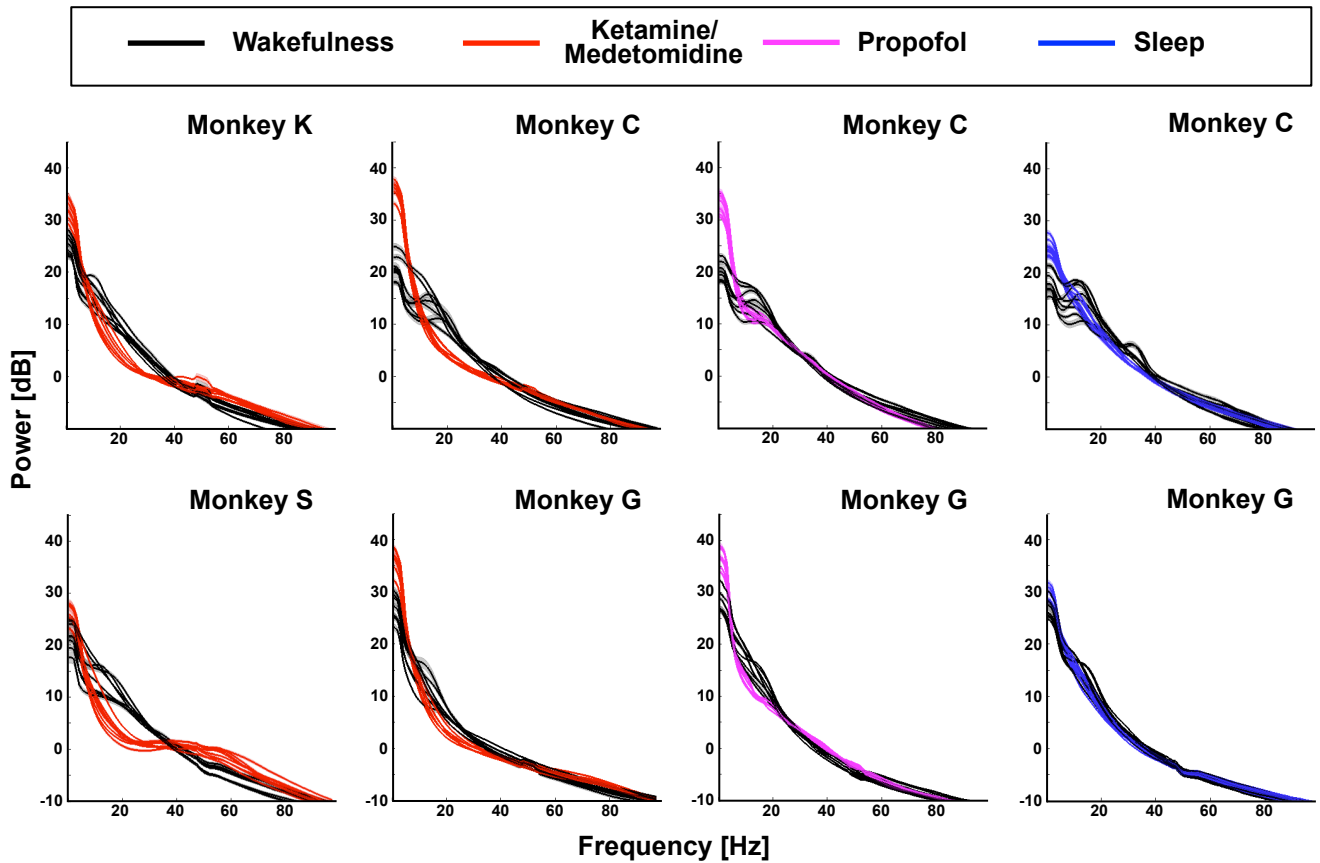
Supplementary Fig. 7

Spatial patterns of ECoG power co-variation at different frequency bands during (a) the propofol anesthesia and (b) sleep.



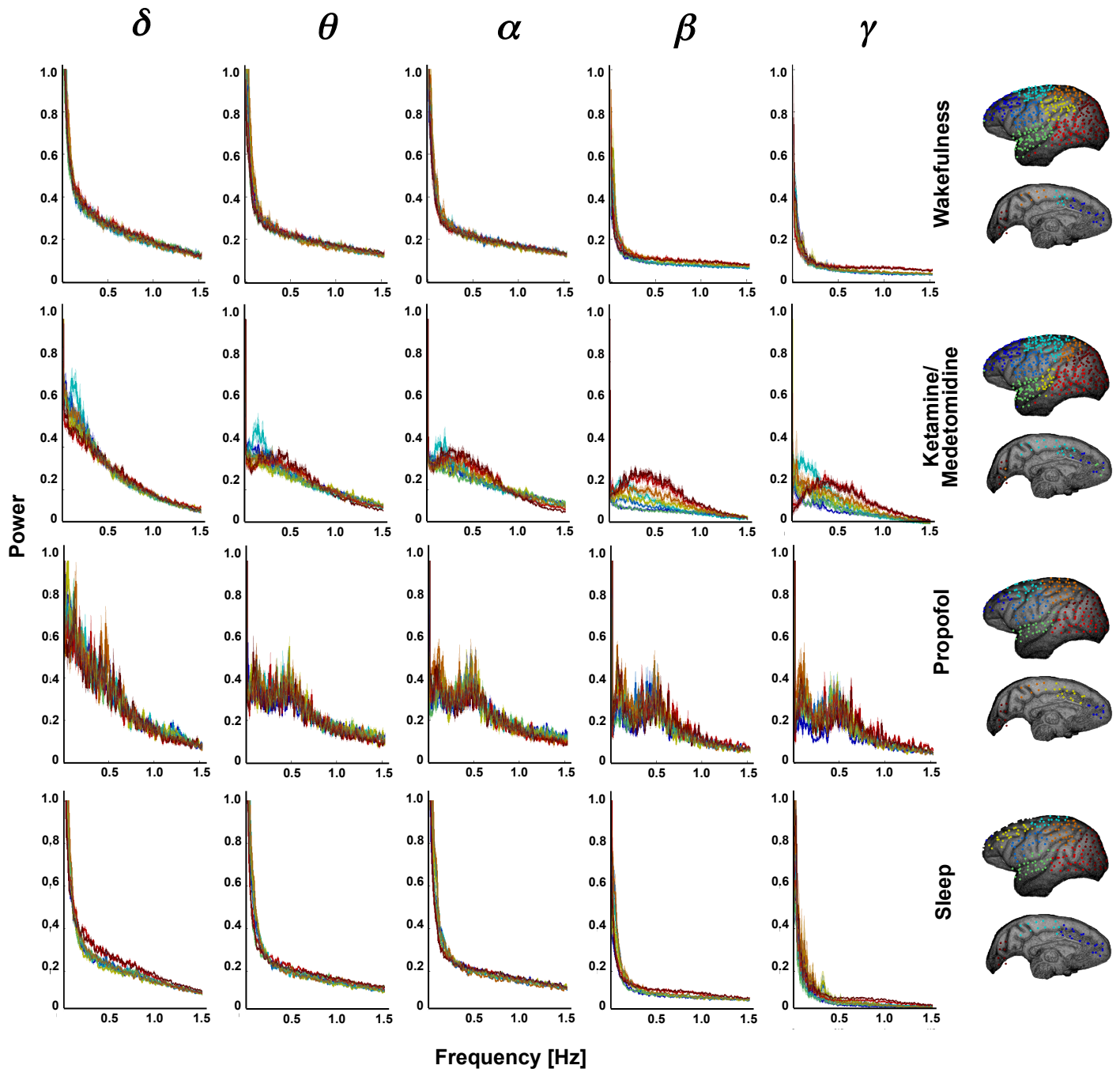
Supplementary Fig. 8

ECoG raw signals, power spectra, and spatial patterns of broadband ECoG power co-variation during the propofol anesthesia and sleep. (a) Similar to the ketamine/medetomidine anesthesia (**Fig 2b,c**), ECoG signals of the two exemplary electrodes (**Fig 2a**) were also characterized by low-frequency, large-amplitude voltage pattern during the propofol anesthesia and sleep, whose power spectra are also significantly different from that of the waking condition. (b) However, the spatial patterns of the broadband ECoG power co-variations remain largely similar. The ECoG were recorded for these two conditions only from Monkey C and G, whose electrodes did not cover some areas in the temporal lobe (**Fig 2a**); and the differences in coverage may partly contribute to differences in spatial patterns between these two conditions and the eyes-closed wakefulness and ketamine/medetomidine anesthesia.



Supplementary Fig. 9

Network-specific power spectra seen at single experiments. The analysis in Fig 5 was repeated on 8 representative experiments from all 4 monkeys. The power spectra (demeaned) consistently show much larger cross-network variations under the eyes-closed wakefulness (black) than during the ketamine/medetomidine anesthesia (red), propofol anesthesia (magenta), and sleep (blue). Different lines are spectra for different networks (clusters), and shadows represent areas within one S.E.M. across electrodes with the same network. Monkey G appeared to be drowsy even during the eyes-closed wakefulness in the sleep experiment by showing significant higher sleep score (0.146 ± 0.089 , Mean \pm SD; compared to 0.048 ± 0.034 in Monkey C under the same condition; $P = 3 \times 10^{-311}$, two sample t-test), and this may explain the small cross-network variations in corresponding spectra (black, the second row of the last column).



Supplementary Fig. 10

Power spectra of band-limited powers (BLPs) in different clusters under various conditions. During the eyes-closed wakefulness (top) and sleep (bottom), the temporal variation of the BLPs is mainly under 0.1 Hz without any obvious oscillatory components; while during the anesthesia (the middle two rows), the relatively periodic fluctuations around 0.2–0.5 Hz are evident by corresponding bumps in the spectra. Shadows represent areas within one S.E.M. across experiments.